Toward a More Detailed Understanding of Oxidative-Addition Mechanisms: Combined Experimental and Quantum-Chemical Study of the Insertion of Titanium Atoms into C−H, Si−H, and Sn−H Bonds

Angela Bihlmeier,[†] Tim M. Greene,[‡] and Hans-Jörg Himmel*[,†]

Institut für Anorganische Chemie, Universität Karlsruhe, Engesserstrasse, Geb. 30.45, 76128 Karlsruhe, Germany, and Department of Chemistry, University of Exeter, Stocker Road, Exeter EX4 4QD, U.K.

Received February 11, 2004

The reactions between Ti atoms and CH_4, SiH_4, and SnH_4 at a temperature of 12 K in Ar matrixes were studied experimentally by IR spectroscopy, taking in the effect of isotopic substitution, and by quantum-chemical calculations. The experiments show that the reactivity changes considerably from CH_4 to SiH_4 or SnH_4. The reaction between Ti and CH_4 proceeds inefficiently, and only after photolytic activation of the Ti atoms does insertion occur to give $HTiCH_3$, which features only terminal Ti−H and C−H bonds. On the other hand, reactions with SiH_4 and SnH_4 occur upon deposition, leading to the products *cis*- and *trans*-$HTi(\mu\text{-}H)_2SiH$ and $HTi(\mu\text{-}H)_3E$ (E = Si, Sn). Selective photolysis can be used to increase the yields of these products. In agreement with the experimental results, quantum-chemical calculations predict the lowest energy form of a molecule with the overall formula $TiEH_4$ to be $HTiCH_3$ with only terminal H atoms for E = C but $HTi(\mu\text{-}H)_3E$ with three bridging H atoms in the case of E = Si, Sn.

Introduction

Oxidative addition is an important reaction, representing a key step in many catalytic cycles. However, the mechanisms of these processes are not fully understood. The activation of C−H bonds is of particular importance. It may be expected that oxidative addition proceeds via a complex, which has in the case of derivatives of silane or methane ($HSiR_3$ and HCR_3) the formulas $L_nM{\cdot}SiHR_3$ and $L_nM{\cdot}CHR_3$, respectively, where L represents a ligand and M the metal center. Several complexes of SiH_4 and even a few of CH_4 have been successfully characterized. Examples include the complex $[Mo(\eta^2\text{-}SiH_4)(CO)(R_2PC_2H_4PR_2)_2]$ (R = Ph, ^{i}Bu, Et), which is apparently in thermal equilibrium with the product of oxidative addition, viz. $[Mo(H)SiH_3(CO)(R_2PC_2H_4PR_2)_2]$.[1]

Complexes featuring BH_4^- groups have also been the subject of much study. The BH_4^- unit is isoelectronic with CH_4, and therefore, it has been argued that the characterization of the structure, bonding, and conformational variations displayed by derivatives of the BH_4^- anion may hold vital clues to C−H activation processes. The compound $Ti(BH_4)_3$ has been characterized in the gas phase via electron diffraction and UV photoelectron spectroscopy and by IR spectroscopy of the matrix-isolated molecule.[2]

Several other species with Ti centers show that the coordination mode of the BH_4^- unit may vary. Thus, the

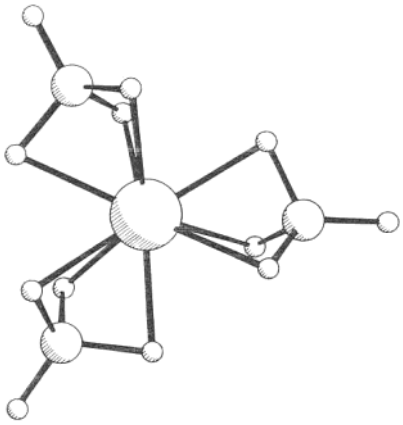

$Ti(BH_4)_3$

compound $Ti(BH_4)_3(PMe_3)_2$, for example, features a side-on coordination of the Ti center to one of the B−H bonds in each of two BH_4^- groups, while the third BH_4^- group adopts a η^2 coordination mode.[3] Another example is the compound $Ti(BH_4)_2(dmpe)_2$ (dmpe = $(CH_3)_2PCH_2CH_2P(CH_3)_2$), in which two η^2-coordinated BH_4^- units are present.[4]

There have been numerous previous studies of the interaction of methane with transition-metal atoms, e.g. Fe,[5] Co,[6,7] and Ni,[8,9] to name only a few examples (see also ref 10 and references therein). The reactions of

* To whom correspondence should be addressed. Fax: +49-721-608-4854. E-mail: himmel@chemie.uni-karlsruhe.de.
[†] Universität Karlsruhe.
[‡] University of Exeter.

(1) Luo, X.-L.; Kubas, G. J.; Burns, C. J.; Bryan, J. C.; Unkefer, C. J. *J. Am. Chem. Soc.* **1995**, *117*, 1159.
(2) (a) Dain, C. J.; Downs, A. J.; Rankin, D. W. H. *Angew. Chem.* **1982**, *94*, 557. (b) Dain, C. J.; Downs, A. J.; Goode, M. J.; Evans, D. G.; Nicholls, K. T.; Rankin, D. W. H.; Robertson, H. E. *J. Chem. Soc., Dalton Trans.* **1991**, 967.
(3) Jensen, J. A.; Girolami, G. S. *J. Chem. Soc., Chem. Commun.* **1986**, 1160.

10.1021/om040016o CCC: $27.50
Publication on Web 04/15/2004

Zn,[11,12] Cd,[12] and Hg[12,13] atoms with CH_4 in Ar and CH_4 matrixes have also been studied, as have those between the main-group atoms Mg,[14] B,[15] Al,[16,17] Ga,[18] and In[18c] and CH_4. In all cases, a species of the form $HMCH_3$ with a terminal M−H bond and a methyl group featuring terminal C−H bonds is formed, but the reaction proceeds only after photoactivation of the metal atom. In previous studies some of us have explored the reactions of the group 13 element atoms Al and Ga with SiH_4;[19,20] in both cases, a spontaneously formed complex featuring a η^2-coordinated metal atom was identified and characterized.

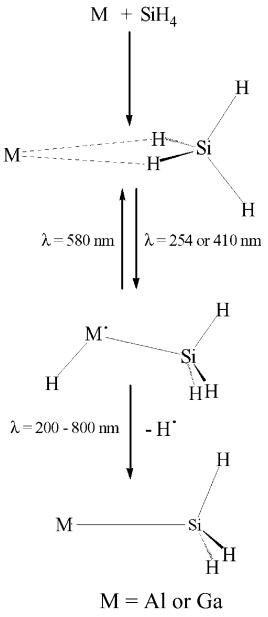

M = Al or Ga

The data allowed for an estimate of the differences in the bond distances d(Si−H) of the slightly distorted SiH_4 unit. On photolytic activation, the metal atoms inserted into the Si−H bond to give $HAlSiH_3$ and $HGaSiH_3$. In these products, again only terminal H atoms are present. The reaction of the photoexcited group 12 metals with SiH_4 yields also the insertion products $HMSiH_3$.[21]

Finally, mechanisms leading to oxidative addition have also been studied in the gas phase by a variety of different techniques. The insertion of metal ions was analyzed, for example, by mass spectrometry, and in some celebrated cases it has proved possible to determine dissociation energies for certain of the species that are generated.[22] One important result of these studies is that most transition metals (charged or uncharged) cannot easily be persuaded to react with methane. In the case of some metals, e.g. rhodium,[23] not only the possible reaction of the metal atom cation but also the reactions of the positively charged dimer and of small clusters were analyzed. An interesting outcome is that Rh_2^+ reacts spontaneously with CH_4 to give the dehydrogenation product $[Rh_2CH_2]^+$, but Rh^+ and Rh_n^+ clusters ($n \geq 2$) do not show this behavior.

Herein we report on the reactions occurring between Ti atoms and CH_4, SiH_4, and SnH_4. In a future publication we will report our investigations on the reactions of Ni atoms with SiH_4 and SnH_4.[24] Hence, it will be shown that the structures of the products of the spontaneous and photolytically activated reactions between Ti atoms and SiH_4 or SnH_4 differ significantly from those of other MEH_4 species that have been studied to date.

Experimental Section

Evaporation of Ti metal was achieved from a resistively heated Ti filament. The amount of deposited metal was monitored by using a microbalance and by UV/vis spectroscopy. UV/vis and Raman spectroscopy were also used to obtain information about the amount of metal dimers present in the matrix.[25] The matrix was deposited on a freshly polished Cu block cooled to 12 K by means of a closed-cycle refrigerator (Leybold LB 510). Other details of the matrix-isolation technique can be found elsewhere.[26]

SiH_4 was used as purchased from Linde (purity >99.99%). SiD_4, SnH_4, and SnD_4 were prepared by the reaction of $SiCl_4$ or $SnCl_4$ with $LiAlH_4$ or $LiAlD_4$ in diglyme and purified by fractional condensation in vacuo. Argon was used as delivered from Messer (purity 99.998%).

IR spectra were recorded with a Bruker 113v spectrometer. An MCT detector was used for the spectral region 4000−650 cm^{-1}. Measurements in the region 700−200 cm^{-1} were carried out with a DTGS detector. Additional spectra between 700 and 50 cm^{-1} were recorded using a liquid He cooled bolometer.

UV/vis spectra were recorded with a Xe arc lamp (Oriel), an Oriel Multispec spectrograph, and a photodiode-array detector. The resolution varied between 0.2 and 0.5 nm.

A Hg medium-pressure lamp (Philips LP125) in combination with interference filters was used for photolysis of the matrixes.

Quantum-chemical calculations were carried out with the TURBOMOLE program.[27] The BP method in combination with an SVP basis set was used for Ti, Si, and H. In the case of Sn,

(4) Jensen, J. A.; Wilson, S. R.; Schultz, A. J.; Girolami, G. S. *J. Am. Chem. Soc.* **1987**, *109*, 8094.
(5) Kauffman, J. W.; Hauge, R. H.; Margrave, J. L. *High Temp. Sci.* **1984**, *17*, 237.
(6) Billups, W. E.; Chang, S.-C.; Hauge, R. H.; Margrave, J. L. *J. Am. Chem. Soc.* **1993**, *115*, 2039.
(7) Billups, W. E.; Chang, S.-C.; Hauge, R. H.; Margrave, J. L. *J. Am. Chem. Soc.* **1995**, *117*, 1387.
(8) Chang, S.-C.; Hauge, R. H.; Billups, W. E.; Margrave, J. L.; Kafafi, Z. H. *Inorg. Chem.* **1988**, *27*, 205.
(9) Himmel, H.-J. *Chem. Eur. J.*, in press.
(10) Ozin, G. A.; McCaffrey, J. G.; Parnis, J. M. *Angew. Chem., Int. Ed.* **1986**, *25*, 1072.
(11) Billups, W. E.; Konarski, M. M.; Hauge, R. H.; Margrave, J. L. *J. Am. Chem. Soc.* **1980**, *102*, 7393.
(12) Greene, T. M.; Andrews, L.; Downs, A. J. *J. Am. Chem. Soc.* **1995**, *117*, 8180.
(13) (a) Legay-Sommaire, N.; Legay, F. *Chem. Phys. Lett.* **1994**, *217*, 97. (b) Legay-Sommaire, N.; Legay, F. *Chem. Phys.* **1996**, *211*, 367.
(14) McCaffrey, J. G.; Parnis, J. M.; Ozin, G. A.; Breckenridge, W. H. *J. Phys. Chem.* **1985**, *89*, 4945.
(15) (a) Hassanzadeh, P.; Hannachi, Y.; Andrews, L. *J. Phys. Chem.* **1993**, *97*, 6418. (b) Hannachi, Y.; Hassanzadeh, P.; Andrews, L. *J. Phys. Chem.* **1994**, *98*, 6950.
(16) Jeong, G.; Klabunde, K. J. *J. Am. Chem. Soc.* **1986**, *108*, 7103.
(17) Parnis, J. M.; Ozin, G. A. *J. Phys. Chem.* **1989**, *93*, 1204, 1220.
(18) (a) Lafleur, R. D.; Parnis, J. M. *J. Phys. Chem.* **1992**, *96*, 2429. (b) Xiao, Z. L.; Hauge, R. H.; Margrave, J. L. *Inorg. Chem.* **1993**, *32*, 642. (c) Himmel, H.-J.; Downs, A. J.; Greene, T. M.; Andrews, L. *Organometallics* **2000**, *19*, 1060.
(19) Gaertner, B.; Himmel, H.-J. *Angew. Chem.* **2002**, *114*, 1602; *Angew. Chem., Int. Ed.* **2002**, *41*, 1538.
(20) Gaertner, B.; Himmel, H.-J.; Macrae, V. A.; Downs, A. J.; Greene, T. M. *Chem. Eur. J.*, in press.
(21) (a) Legay-Sommaire, N.; Legay, F. *J. Phys. Chem. A* **1998**, *102*, 8759. (b) Macrae, V. A.; Greene, T. M.; Downs, A. J. *J. Phys. Chem. A* **2004**, *108*, 1393.
(22) See, for example: Schwarz, H. *Angew. Chem.* **2003**, *42*, 4442 and references given therein.
(23) Albert, G.; Berg, C.; Beyer, M.; Achatz, U.; Joos, S.; Niedner-Schatteburg, G.; Bondybey, V. E. *Chem. Phys. Lett.* **1997**, *268*, 235.
(24) Himmel, H.-J. Unpublished results.
(25) Himmel, H.-J.; Bihlmeier, A. *Chem. Eur. J.* **2004**, *10*, 627.
(26) See, for example: Himmel, H.-J.; Downs, A. J.; Greene, T. M. *Chem. Rev.* **2002**, *102*, 4191.

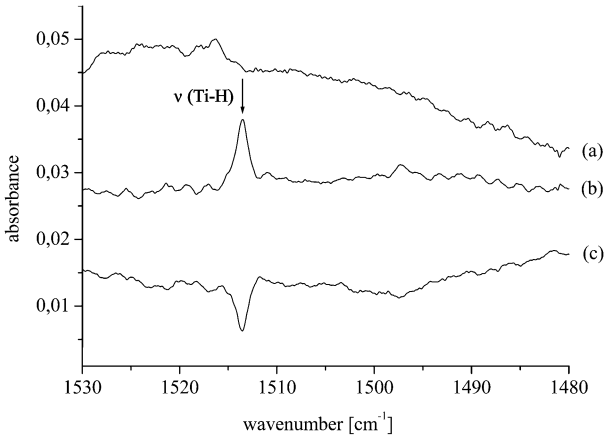

Figure 1. IR spectra in the region around 1500 cm^{-1} recorded for the reaction of Ti atoms with CH_4: (a) spectrum upon deposition; (b) difference between the spectra before and after photolysis at 500 nm; (c) difference between the spectra before and after UV−vis photolysis ($200 < \lambda < 800$ nm).

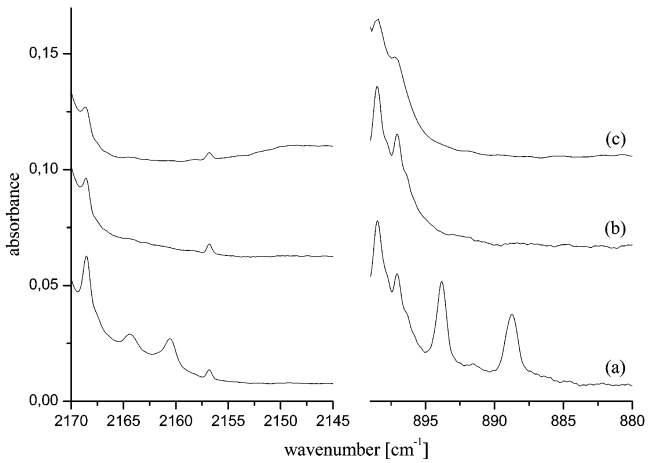

Figure 2. IR spectra in the regions 2170−2145 and 900−880 cm^{-1} of an Ar matrix containing Ti atoms and 0.2% SiH_4: (a) upon deposition; (b) after photolysis at $\lambda_{max} = 500$ nm; (c) after photolysis at $\lambda_{max} = 410$ nm.

an SVP basis set was used only for the two 5s and the two 5p electrons; for the remaining 46 electrons a relativistic ECP (MEFIT, WB)[28] was applied.

Results

In the following account, the results of the experiments involving codeposition of Ti atoms with CH_4, SiH_4, and SnH_4 will be reported in turn.

Ti + CH_4. The spectrum taken following deposition of Ti atoms together with 2% CH_4 in Ar gave no evidence for an absorption due to a product of any reaction between the two reagents (see Figure 1). Subsequently, the matrix was photolyzed with $\lambda_{max} = 500$ nm light for a period of 30 min. This wavelength can initiate a $z(^3D_1) \leftarrow a(^3F_2)$ or a $z(^3F_2) \leftarrow a(^3F_2)$ transition of the Ti atoms.[25,29] The treatment brought about the appearance of a weak but sharp band at 1513.5 cm^{-1}, which can be assigned to the product **1**, from the reaction between Ti and CH_4. Subsequently, the matrix was subjected to a period of 10 min of photolysis with $\lambda_{max} = 410$ nm, resulting in a decrease of the band due to product **1**. No product of the decomposition of **1** was detected. The spectra gave also evidence for weak absorptions due to TiO_2 and H_2TiO.[30]

The experiment was repeated, but with CD_4 in place of CH_4. Again the spectrum taken following deposition showed no sign of any reaction product. Upon photolysis at 500 nm, a weak and sharp band was seen to grow in at 1092.1 cm^{-1}. The absorber responsible for this band is in all probability the perdeuterated version of **1**. The behavior of the band toward further photolysis at a different wavelength was similar to that reported for CH_4. Thus, photolysis at $\lambda_{max} = 410$ nm or broad-band photolysis led to the rapid decay of **1**. Unfortunately, all attempts to increase the yield of **1** (e.g. by increasing the CH_4 or Ti concentrations) failed. We conclude that the reaction between Ti and CH_4 needs activation and proceeds inefficiently under the conditions of our experiments to give a low product yield.

Ti + SiH_4. Unlike the experiments with CH_4, the IR spectrum taken upon deposition of Ti atoms together with SiH_4 gave evidence for spontaneously formed reaction products. Several experiments showed that not one but four species are formed immediately upon deposition. Selective photolysis proved to be extremely useful to discriminate between these different species. First, a family of absorptions appeared at 2164.3, 2160.4, 893.8, and 888.7 cm^{-1}. These wavenumbers are close to those of free SiH_4, and thus, low concentrations of SiH_4 (0.2%) in the matrix were necessary in order to observe all of them (see Figure 2). The bands decrease sharply upon photolysis at $\lambda_{max} = 500$ nm and were completely extinguished by photolysis employing broad-band visible light ($400 < \lambda < 800$ nm). The source of these absorptions is in all probability a complex of the form Ti·SiH_4.

Some of the bands observed for the remaining three species have very similar wavenumbers (see Figure 3). Thus, there should be some similarities in the structures of these species. Especially close were the bands of two products, which will be referred to as **2aa** and **2ab** in the following discussion. The bands of **2aa** and **2ab** also show almost the same response to the various photolysis cycles. Thus, the bands increase on brief photolysis at $\lambda_{max} = 500$ (1 min) and decrease on photolysis at $\lambda_{max} = 410$. **2aa** has bands centered at 2055.0/2047.4, 1541.5, 1507.2, 1144.5, and 854.0 cm^{-1} and **2ab** at 2042.5/2040.5, 1514.1, 1120.7, and 937.8/934.2 cm^{-1}.

The bands belonging to the fourth species, **3a**, appear at 1524.8, 1509.2, 1498.1, and 1129.7 cm^{-1}. They can easily be distinguished from the bands of **2aa** and **2ab** on the basis of their response to photolysis. Thus, the bands of species **3a** were seen to grow upon photolysis at $\lambda_{max} = 410$ at the expense of those due to **2aa** and **2ab**. The obvious inference is that **2aa** and **2ab** are precursors to **3a**.

The bands due to **3a** decreased slowly upon photolysis of the matrix with broad-band visible light ($400 < \lambda <$

(27) Ahlrichs, R.; Bär, M.; Häser, M.; Horn, H.; Kölmel, C. *Chem. Phys. Lett.* **1989**, *162*, 165. Eichkorn, K.; Treutler, O.; Öhm, H.; Häser, M.; Ahlrichs, R. *Chem. Phys. Lett.* **1995**, *240*, 283. Eichkorn, K.; Treutler, O.; Öhm, H.; Häser, M.; Ahlrichs, R. *Chem. Phys. Lett.* **1995**, *242*, 652. Eichkorn, K.; Weigend, F.; Treutler, O.; Ahlrichs, R. *Theor. Chem. Acc.* **1997**, *97*, 119. Weigend, F.; Häser, M. *Theor. Chem. Acc.* **1997**, *97*, 331. Weigend, F.; Häser, M.; Patzelt, H.; Ahlrichs, R. *Chem. Phys. Lett.* **1998**, *294*, 143.
(28) Bergner, A.; Dolg, M.; Kuechle, W.; Stoll, H.; Preuss, H. *Mol. Phys.* **1993**, *80*, 1431.
(29) Gruen, D. M.; Carstens, D. H. W. *J. Chem. Phys.* **1971**, *54*, 5206.
(30) Zhang, L.; Dong, J.; Zhou. M. *J. Phys. Chem. A* **2000**, *104*, 8882.

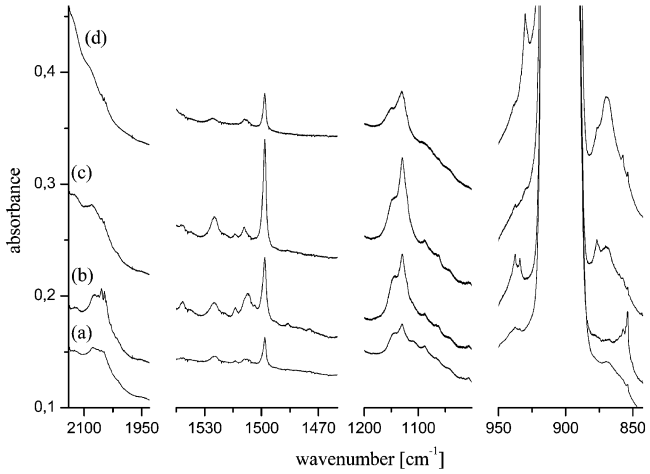

Figure 3. IR spectra recorded for the reaction of Ti atoms with SiH_4: (a) upon deposition; (b) after photolysis at λ_{max} = 500 nm; (c) after photolysis at λ_{max} = 410 nm; (d) after broad-band visible photolysis (400 < λ < 800 nm).

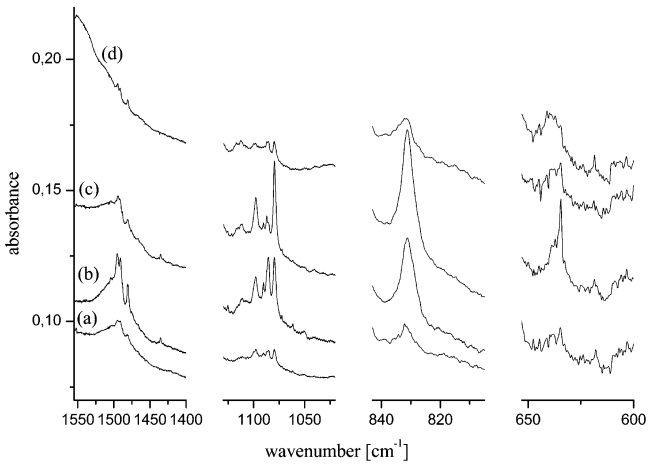

Figure 4. IR spectra recorded for the reaction of Ti atoms with SiD_4: (a) upon deposition; (b) after photolysis at λ_{max} = 500 nm; (c) after photolysis at λ_{max} = 410 nm; (d) after broad-band visible photolysis (400 < λ < 800 nm).

800 nm). A weak but sharp absorption at 930.2 cm^{-1} and a broad one around 869 cm^{-1} appeared upon prolonged photolysis.

The experiment was repeated with SiD_4 in place of SiH_4. First, experiments were conducted with a low percentage of SiD_4 (0.3%) in the matrix. Here, only one band at 657.3 cm^{-1}, which could be assigned to a Ti·SiD_4 complex, was observed upon deposition. This band again decreased sharply upon photolysis at λ_{max} = 500 nm and disappeared completely on further photolysis. Figure 4 displays the spectra taken in an experiment involving a larger concentration of SiD_4 (1.5%), following the same pattern as observed for the reaction with SiH_4. However, the bands due to **2aa** and **2ab** were more clearly visible and the relative intensities of the bands due to product **3a** appeared to be reduced on deposition and after brief photolysis at λ_{max} = 500 nm. All bands were *red*-shifted with respect to the corresponding features observed in the experiments relying on SiH_4. Species **2aa** appeared now in absorptions at 1495.5/1490.8, 1125.6, 1085.6, 829.3, and 634.7 cm^{-1}. Unfortunately, only two bands due to species **2ab** in its perdeuterated version were traced; these appeared at 1480.5 and 1090.5 cm^{-1}.

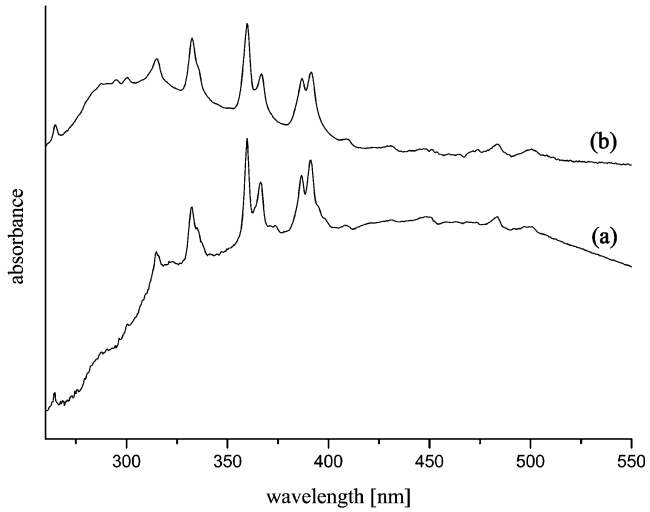

Figure 5. UV/vis spectra of a matrix containing (a) only Ti atoms and (b) Ti atoms together with 1% SiH_4.

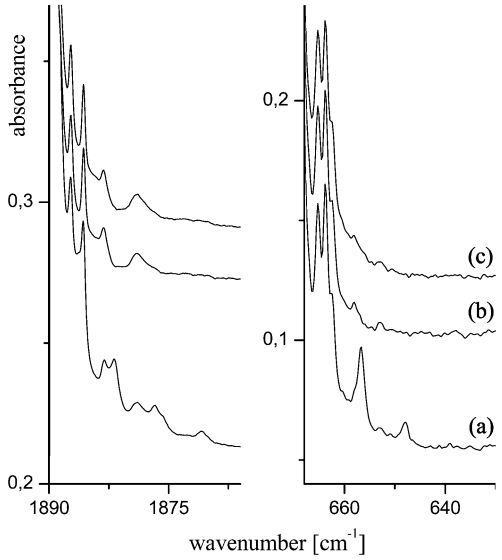

Figure 6. IR spectra in the regions 1890−1860 and 670−650 cm^{-1} of an Ar matrix containing Ti atoms and 0.2% SnH_4: (a) upon deposition; (b) after photolysis at λ_{max} = 500 nm; (c) after photolysis at λ_{max} = 410 nm.

Finally, bands at 1098.3, 1087.2, 1079.7, and 831.3 cm^{-1} can be assigned to product **3a** in its perdeuterated form. Again, these absorptions decreased upon photolysis with broad-band visible light.

In further experiments a bolometer was used to detect bands in the region 700−50 cm^{-1}. However, no bands arising from reaction products were observed in these experiments. Finally, the experiment was repeated with SiD_3H. All absorptions of products **2aa**, **2ab**, and **3a** in their various isotopic forms together with their response toward photolysis are included in Table 1.

Figure 5 displays a UV/vis spectrum of a matrix containing Ti atoms and SiH_4 together with that of a matrix containing only Ti atoms. Unfortunately, it was not possible to detect an absorption arising from one of the products. Nevertheless, it can be seen that the half-width of the absorptions arising from electronic transitions of the Ti atoms slightly increase in the presence of SiH_4. It also can be seen that conditions were chosen for which the concentration of Ti_2 dimers must be very

Table 1. Observed Wavenumbers (cm^{-1}) following the Reaction between Ti Atoms and SiH_4, SiD_4, and SiD_3H

				photolysis			
SiH_4	SiD_4	SiD_3H	deposition	500 nm	410 nm	400−800 nm	absorber
2164.3		2164.0	↑	↓	↓	↓	Ti·SiH_4
2160.4		2160.1	↑	↓	↓	↓	Ti·SiH_4
		1560.3					
2055.0/2047.4		2116.2	↑	↑	↓	↓	*cis*-HTi(μ-H)$_2$SiH (**2aa**)
		2041.7					
	1480.5	1479.8					
2042.5/2040.5		2095.2	↑	↑	↓	↓	*trans*-HTi(μ-H)$_2$SiH (**2ab**)
	1495.5/1490.8	1495.9/1491.4					
1541.5	1125.6		↑	↑	↓	↓	*cis*-HTi(μ-H)$_2$SiH (**2aa**)
1524.8		1525.5	↑	↑	↑	↓	HTi(μ-H)$_3$Si (**3a**)
	1098.3	1102.5/1098.4					
1514.1	1090.5	1090.5	↑	↑	↓	↓	*trans*-HTi(μ-H)$_2$SiH (**2ab**)
1509.2	1087.2		↑	↑	↑	↓	HTi(μ-H)$_3$Si (**3a**)
1507.2		1508.4	↑	↑	↓	↓	*cis*-HTi(μ-H)$_2$SiH (**2aa**)
	1085.6	1086.4					
1498.1		1498.3	↑	↑	↑	↓	HTi(μ-H)$_3$Si (**3a**)
	1079.7	1079.0					
1144.5	829.3		↑	↑	↓	↓	*cis*-HTi(μ-H)$_2$SiH (**2aa**)
1129.7	831.3	1150.5	↑	↑	↑	↓	HTi(μ-H)$_3$Si (**3a**)
1120.7			↑	↑	↓	↓	*trans*-HTi(μ-H)$_2$SiH (**2ab**)
937.8/934.2			↑	↑	↓	↓	*trans*-HTi(μ-H)$_2$SiH (**2ab**)
893.8		839.5	↑	↓	↓	↓	Ti·SiH_4
		838.9					
888.7	657.3	657.7	↑	↓	↓	↓	Ti·SiH_4
		637.6					
877.3				↑	↑	↓	*trans*-HTi(μ-H)$_2$SiH (**2ab**)
854.0	634.7		↑	↑	↓	↓	*cis*-HTi(μ-H)$_2$SiH (**2aa**)

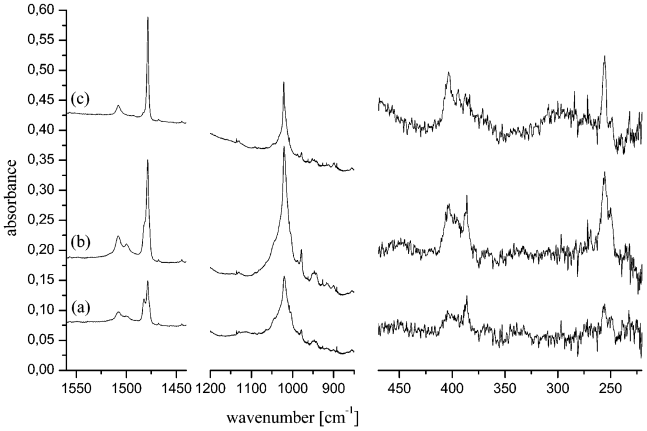

Figure 7. IR spectra recorded for the reaction of Ti atoms with SnH_4: (a) upon deposition; (b) after photolysis at λ_{max} = 500 nm; (c) after broad-band visible photolysis (400 < λ < 800 nm).

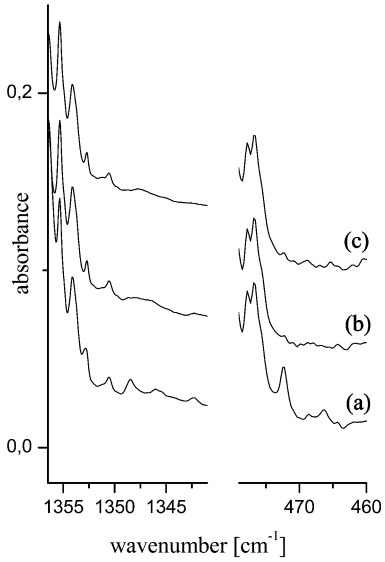

Figure 8. IR spectra in the regions 1355−1340 and 480−460 cm^{-1} of an Ar matrix containing Ti atoms and 0.2% SnD_4: (a) upon deposition; (b) after photolysis at λ_{max} = 500 nm; (c) after photolysis at λ_{max} = 410 nm.

low. The absorptions characteristic for Ti_2 are not present under these conditions.[25] Thus, we can role out the involvement of Ti_2 in the reactions.

Ti + SnH_4. Upon deposition of an Ar matrix containing Ti atoms and SnH_4, IR bands at 1881.8, 1876.7, 1870.7, 657.0, and 648.0 cm^{-1} were observed to arise from the first, spontaneously formed product, which is most likely to be a complex of the form Ti·SnH_4. The absorptions of this complex are close to the bands of SnH_4. Therefore, with higher concentrations of SnH_4 in the matrix (1.5%), some of the bands were hidden under the stronger bands of free SnH_4 and could be discerned only when lower concentrations of SnH_4 (0.2%) were used. The bands of the complex decreased sharply following photolysis with light having λ_{max} = 500 nm and disappeared completely upon broad-band visible radiation (see Figure 6).

Additional features were observed at 1499.6, 1482.4, 1043.4, 978.5, 385.9, and 249.7 cm^{-1}, and these can be assigned to the two absorbers **4ba** and **4bb**. Since all the absorptions of **4ba** are close to those of **4bb** (see Figure 7), it is reasonable to assume that **4ba** and **4bb** must have very similar structures. It is therefore difficult to assign the bands to one or the other of these two species. However, on the basis of several experiments we have assigned the bands at 1482.4, 1043.4, and 385.9 cm^{-1} to species **4ba** and those at 1499.6, 978.5, and 249.7 cm^{-1} to **4bb**. We note that the absorptions at 1499.6 and 1482.4 cm^{-1} have wavenumbers suggestive of ν(Ti−H) fundamentals. The bands grew

Table 2. Observed Wavenumbers (in cm^{-1}) Following the Reaction between Ti Atoms and Stannane (SnH_4 and SnD_4)

			photolysis			
SnH_4	SnD_4	deposition	500 nm	410 nm	400−800 nm	absorber
1881.8	1348.5	↑	↓	↓	↓	Ti·SnH_4
1876.7	1345.9	↑	↓	↓	↓	Ti·SnH_4
1870.7	1342.4	↑	↓	↓	↓	Ti·SnH_4
1508.1		↑	↑	↑	↑	$HTi(\mu\text{-}H)_3Sn$ (**3b**)
1499.6	1080.6	↑	↑	↓	↓	$HTi(\mu\text{-}H)_2(H)Sn$ (**4bb**)
1482.4	1069.0	↑	↑	↓	↓	$HTi(\mu\text{-}H)_2(H)Sn$ (**4ba**)
1478.4	1065.0	↑	↑	↑	↑	$HTi(\mu\text{-}H)_3Sn$ (**3b**)
1043.4	733.5	↑	↑	↓	↓	$HTi(\mu\text{-}H)_2(H)Sn$ (**4ba**)
1021.2		↑	↑	↑	↑	$HTi(\mu\text{-}H)_3Sn$ (**3b**)
1016.5	741.3	↑	↑	↑	↑	$HTi(\mu\text{-}H)_3Sn$ (**3b**)
978.5		↑	↑	↓	↓	$HTi(\mu\text{-}H)_2(H)Sn$ (**4bb**)
	939.9	↑	↑	↑	↑	$HTi(\mu\text{-}H)_3Sn$ (**3b**)
	905.5	↑	↑	↑	↑	$HTi(\mu\text{-}H)_3Sn$ (**3b**)
657.0	472.3	↑	↓	↓	↓	Ti·SnH_4
648.0	466.4	↑	↓	↓	↓	Ti·SnH_4
624.8	452.0	↑	↑	↑	↑	$HTi(\mu\text{-}H)_3Sn$ (**3b**)
385.9		↑	↑	↓	↓	$HTi(\mu\text{-}H)_2(H)Sn$ (**4ba**)
255.8		↑	↑	↑	↑	$HTi(\mu\text{-}H)_3Sn$ (**3b**)
249.7		↑	↑	↓	↓	$HTi(\mu\text{-}H)_2(H)Sn$ (**4bb**)
	183.2	↑	↑	↑	↑	$HTi(\mu\text{-}H)_3Sn$ (**3b**)

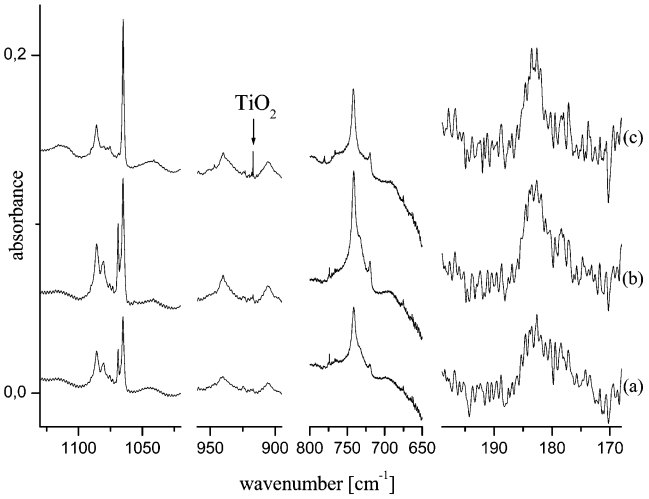

Figure 9. IR spectra recorded for the reaction of Ti atoms with SnD_4: (a) upon deposition; (b) after photolysis at λ_{max} = 500 nm; (c) after photolysis at λ_{max} = 410 nm; (d) after broad-band visible photolysis (400 < λ < 800 nm).

on photolysis at λ_{max} 500 nm and decreased when the matrix was irradiated with broad-band visible light.

Finally, a family of bands located at 1508.1, 1478.4, 1021.2, 1016.5, 624.8, and 255.8 cm^{-1} belong to the species **3b** (see Figure 7). The strong band at 1478.4 cm^{-1} and the weak one at 1508.1 cm^{-1} again appear in a region characteristic of ν(Ti−H) fundamentals, whereas the absorptions at 1021.2 and 1016.5 cm^{-1} argue for the presence of bridging H atoms. The behavior of these bands toward photolysis was distinctly different from the behavior observed for products **4ba** and **4bb**. Thus, the bands grew on λ_{max} = 500 nm photolysis and remained almost unchanged when the matrix was irradiated with broad-band visible light.

Additional experiments were conducted with SnD_4. The bands of the Ti·SnD_4 complex were now observed at 1348.5, 1345.9, 1342.4, 472.3, and 466.4 cm^{-1} (see Figure 8). The bands due to products **4ba** and **4bb** were *red*-shifted to 1069.0 cm^{-1} (**4ba**), 1080.6 cm^{-1} (**4bb**) and 733.5 cm^{-1} (**4ba**) (see Figure 9). Our experiments gave evidence of six absorptions due to product **3b**. These were located at 1065.0, 939.9, 905.5, 741.3, 452.0, and 183.2 cm^{-1}. The photolysis behavior of all the species is the same as that observed in the experiments with SnH_4.

Table 2 includes all the absorptions assignable to the TiSnH_4(SnD_4) contact pair and the products **3b**, **4ba**, and **4bb** of the reactions of Ti atoms with SnH_4 and SnD_4.

Discussion

The results clearly show that the product of the reaction with CH_4 differs significantly from those identified in the reactions with either SiH_4 or SnH_4. The observation of at least one absorption in the region characteristic of the stretching vibrations of terminal Ti−H bonds suggests that molecules of the form $HTi(\mu\text{-}H)_nEH_{3-n}$ are formed. On the basis of experiments with several different concentrations of Ti in the matrix and of the UV/vis spectra (see Figure 5), we can rule out that more than one Ti atom is present in the observed reaction products. The spectra also show that n is different for the three reactants CH_4, SiH_4, and SnH_4. Several isomers (structures **A**−**E**) have to be considered for a species with this general formula. We therefore start our discussion with a survey of all the

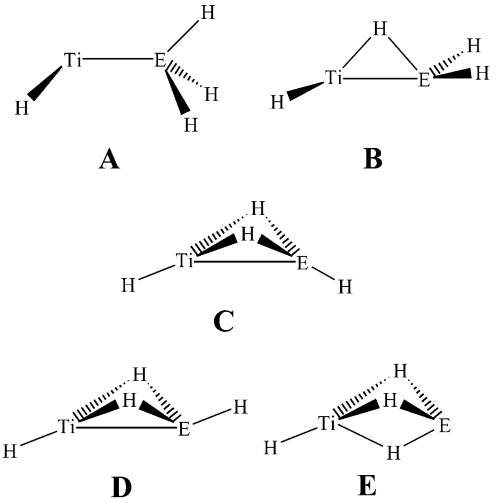

Table 3. Calculated Dimensions (Distances in pm, Angles in deg), IR Properties (Wavenumbers in cm^{-1}, Intensities (in km mol^{-1}) Given in Parentheses). and Relative Energies (in kJ mol^{-1}) for the Singlet, Triplet, and Quintet Electronic States of $HTiCH_3$

	singlet ($^1A'$)	triplet ($^3A''$)	quintet ($^5A'$)
d(Ti−C)	201.9	207.9	230.9
d(Ti−H)	170.5	175.2	185.1
d(C−H)	110.9/111.8/ 111.8	111.2/111.7/ 111.7	110.5/110.5/ 110.9
∠(H−Ti−C)	110.2	119.8	178.9
ν_1(a′)	3068.4 (2)	3039.4 (2)	3107.6 (1)
ν_2(a′)	2889.6 (1)	2899.6 (3)	2945.4 (1)
ν_3(a′)	1641.3 (180)	1551.3 (267)	1337.2 (6)
ν_4(a′)	1300.3 (2)	1336.9 (2)	1227.8 (17)
ν_5(a′)	1031.0 (18)	1069.2 (4)	808.2 (188)
ν_6(a′)	565.8 (69)	568.0 (118)	362.0 (16)
ν_7(a′)	432.1 (9)	467.6 (7)	293.8 (11)
ν_8(a′)	208.6 (15)	279.1 (36)	222.7 (23)
ν_9(a″)	2991.5 (4)	2989.5 (8)	3130.3 (0.001)
ν_{10}(a″)	1334.8 (15)	1345.8 (7)	1293.9 (1)
ν_{11}(a″)	335.5 (6)	357.6 (19)	389.1 (12)
ν_{12}(a″)	184.8 (35)	194.7 (48)	273.8 (0.2)
ΔE	92.7	0	232.5
ΔE_{ZPE}	92.0	0	228.3

possible isomers on the basis of quantum-chemical calculations. The results of this survey will prove to be invaluable in the identification and characterization of the species formed in the course of our experiments.

Quantum-Chemical Calculations: $HTiEH_3$ (A; $n = 0$). The global energy minimum for a molecule with the formula $TiCH_4$ is a species exhibiting a triplet electronic ground state and having one terminal Ti−H (175.2 pm) bond, three terminal C−H bonds (111.2−111.7 pm), and a direct Ti−C bond (207.9 pm). The angle H−Ti−C turns out to be close to 120°. No minimum was found in which one or more of the H atoms occupy a bridging position. Table 3 summarizes the calculated dimensions and IR properties not only for the triplet ground electronic state but also for the lowest energy singlet and quintet electronic states, which are 92 and 228 kJ mol^{-1}, respectively, higher in energy than the ground state. The calculations predict one of the vibrational modes, the ν(Ti−H) stretching fundamental ν_3, to carry most of the intensity. In the case of the singlet electronic state, the Ti−H bond is significantly shorter (170.5 pm) and, as a consequence, the ν(Ti−H) stretching fundamental is predicted to appear at higher wavenumber (1641.3 cm^{-1}). For E = Si, Sn, no minimum could be found for such a structure in which none of the H atoms occupies a bridging position.

$HTi(\mu\text{-}H)EH_2$ (B; $n = 1$). No energy minimum could be found for this isomer when E = C. For E = Si, Sn, however, isomers of this form were located by our calculations. Some dimensions and vibrational properties are summarized in Tables 4 and 5. Both species possess only C_1 symmetry. The Ti−Si and Ti−Sn distances measure 246.5 and 273.9 pm, respectively. This isomer has the highest energy of all the calculated minima. In the case of the Si homologue, the energy difference from the other forms is relatively small, but in the case of the Sn-containing compound this species is already 87.1 kJ mol^{-1} higher in energy than the global minimum form.

***cis*- and *trans*-$HTi(\mu\text{-}H)_2EH$ (C, D; $n = 2$).** Again, energy minima of this form were found for E = Si, Sn but not for E = C. The cis and trans forms were found to have similar energies. The cis form is calculated to be slightly more stable, but the energy difference from the trans form amounts to no more than 0.4 and 6.8 kJ mol^{-1} for E = Si, Sn, respectively. In the case of the Si compound, the Ti−Si distance (242.1 pm in the cis form and 236.4 pm in the trans form) is slightly shorter than in the isomer with the structure **B**. In all cases, the Ti−H_t distance increases with respect to those found in the isomers of structure **B**. In the case of E = Si, these isomers are only 24.3 and 24.7 kJ mol^{-1} higher in energy than the global minimum structure. For E = Sn, however, they are energetically less favored.

$HTi(\mu\text{-}H)_3E$ (E; $n = 3$). This isomer, with three bridging H atoms, represents the global energy minimum for a species of this formula and E = Si or Sn. Again, a triplet state is found to be the ground electronic state. The structure is only slightly distorted from C_s symmetry. The Ti···Si and Ti···Sn distances now amount

Table 4. Calculated Dimensions (Distances in pm), IR Properties (Wavenumbers in cm^{-1}, Intensities (in km mol^{-1}) Given in Parentheses), and Relative Energies (in kJ mol^{-1}) for $HTi(\mu\text{-}H)_nSiH_{3-n}$

	isomer			
	B ($n = 1$)	C ($n = 2$, cis)	D ($n = 2$, trans)	E ($n = 3$)
Ti−H_t	175.0	177.6	177.7	176.1
Ti−H_b	200.6	194.4, 194.4	203.3, 203.4	196.1, 199.1, 199.7
Ti−Si	246.5	242.1	236.4	254.4
Si−H_t	151.4, 151.9	152.1	151.1	
Si−H_b	163.0	162.8, 162.8	161.4, 161.4	160.0, 163.2, 163.2
ν_1	2108.6 (99)	2075.6 (149)	2121.7 (105)	1698.2 (79)
ν_2	2076.7 (117)	1575.2 (90)	1641.0 (68)	1557.3 (222)
ν_3	1558.1 (232)	1564.2 (206)	1628.4 (159)	1546.5 (158)
ν_4	1551.3 (218)	1522.3 (424)	1530.8 (404)	1542.3 (148)
ν_5	1018.6 (153)	1171.2 (197)	1045.7 (204)	1129.8 (398)
ν_6	896.7 (99)	1105.2 (1)	986.3 (2)	1083.8 (54)
ν_7	820.7 (31)	814.2 (31)	849.7 (58)	1045.0 (19)
ν_8	484.9 (2)	608.3 (0.01)	564.9 (3)	743.0 (31)
ν_9	414.4 (147)	512.1 (10)	430.5 (6)	721.0 (13)
ν_{10}	314.8 (11)	317.3 (20)	336.8 (30)	361.8 (51)
ν_{11}	277.5 (68)	196.1 (277)	191.7 (240)	256.4 (136)
ν_{12}	214.4 (57)	155.0 (137)	160.4 (130)	232.2 (87)
ΔE	27.5	24.3	24.7	0

Table 5. Calculated Dimensions (Distances in pm), IR Properties (Wavenumbers in cm^{-1}, Intensities (in km mol^{-1}) Given in Parentheses), and Relative Energies (in kJ mol^{-1}) for $HTi(\mu\text{-}H)_nSnH_{3-n}$

	isomer			
	B ($n = 1$)	C ($n = 2$, *cis*)	D ($n = 2$, *trans*)	E ($n = 3$)
sym	C_1	C_s	C_s	C_1
Ti−H_t	176.9	177.5	178.5	179.2
Ti−H_b	193.4	192.5	193.5	195.8, 199.0, 199.3
Ti−Sn	273.9	279.3	276.4	278.0
Sn−H_t	176.7, 177.5	178.8	178.9	
Sn−H_b	199.0	196.4	199.5	191.3, 196.8, 196.9
ν_1	1727.1 (a, 262)	1667.5 (a′, 302)	1661.1 (a′, 310)	1520.0 (a, 484)
ν_2	1704.0 (a, 270)	1534.2 (a′, 442)	1529.9 (a′, 454)	1302.6 (a, 97)
ν_3	1542.1 (a, 376)	1222.7 (a′, 123)	1217.1 (a′, 151)	1207.2 (a, 104)
ν_4	1188.7 (a, 191)	1105.6 (a′, 320)	952.1 (a′, 69)	1166.0 (a, 168)
ν_5	968.4 (a, 223)	685.5 (a′, 55)	680.3 (a′, 77)	1063.3 (a, 457)
ν_6	701.3 (a, 82)	409.4 (a′, 78)	310.9 (a′, 18)	940.5 (a, 154)
ν_7	618.7 (a, 34)	272.8 (a′, 182)	261.3 (a′, 196)	917.5 (a, 47)
ν_8	441.7 (a, 5)	126.8 (a′, 15)	83.9 (a′, 5)	656.1 (a, 41)
ν_9	345.5 (a, 175)	1171.2 (a″, 219)	1159.9 (a″, 246)	559.4 (a, 89)
ν_{10}	272.3 (a, 92)	1043.1 (a″, 137)	960.6 (a″, 51)	254.7 (a, 87)
ν_{11}	196.3 (a, 10)	540.7 (a″, 1)	478.9 (a″, 19)	195.5 (a, 94)
ν_{12}	182.8 (a, 28)	276.7 (a″, 95)	241.9 (a″, 336)	192.0 (a, 141)
ΔE	87.1	50.5	57.3	0

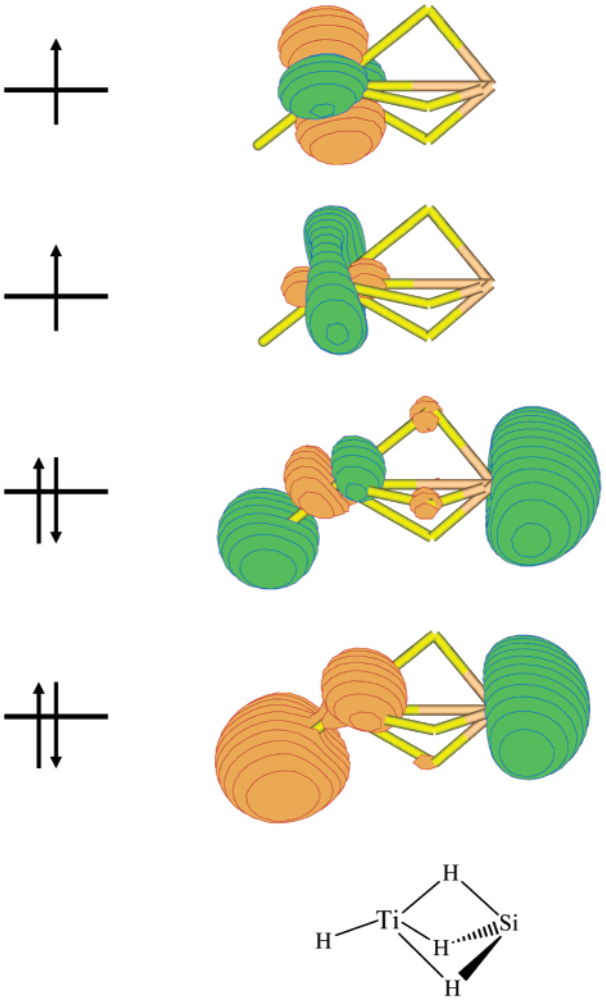

Figure 10. Frontier orbitals of $HTi(\mu\text{-}H)_3Si$.

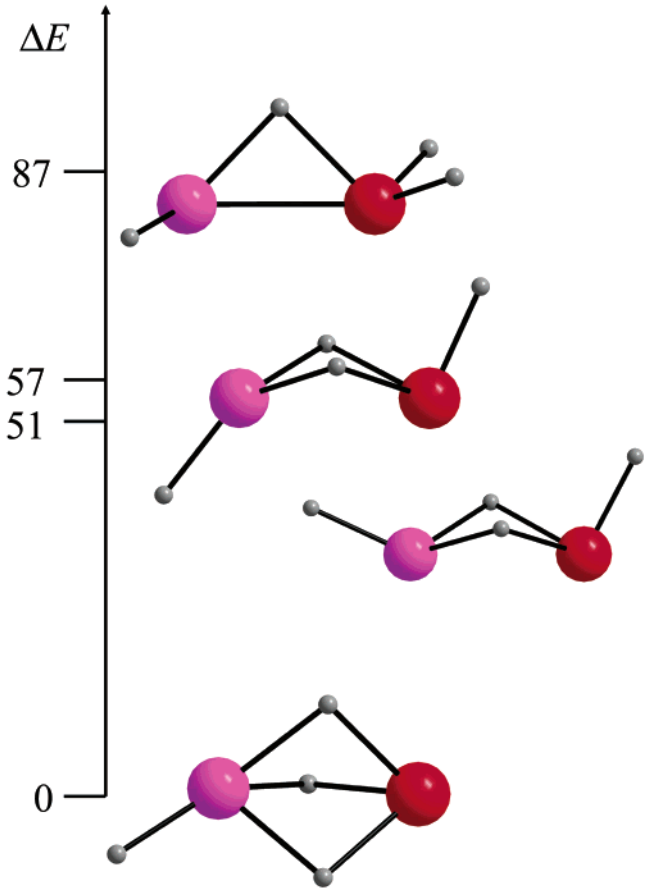

Figure 11. Plot showing the isomers of $TiSnH_4$ and their relative energies.

to 254.4 and 278.0 pm, respectively. The Ti−H_t distance is slightly shorter in $HTi(\mu\text{-}H)_3Si$ (176.1 pm) than it is in $HTi(\mu\text{-}H)_3Sn$ (179.2 pm). Figure 10 displays the frontier orbitals of $HTi(\mu\text{-}H)_3Si$. It can be seen very clearly that the two orbitals that are each occupied by only one electron (SOMO's) are centered at the Ti atom.

Tables 4 and 5 summarize some of the important dimensions, IR properties, and relative energies calculated for isomers **B**−**E** and for E = Si, Sn. Figure 11 shows the minima as calculated by quantum-chemical means in the order of energies for E = Sn.

It is noteworthy, then, that here is an example of a change in structure that occurs between homologues of the first and subsequent rows (in this case from C to Si and Sn). This change of structure is caused by several effects. Certainly the trend in the polarization of the

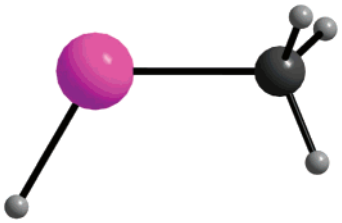

$HTiCH_3$

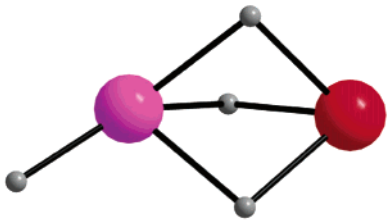

$HTi(\mu\text{-}H)_3Sn$

E−H bonds from CH_4 to SiH_4 and SnH_4 is of importance in this context. The more negatively polarized the H atoms become, the larger the inclination of the Ti atom (acceptor) to establish bonds to them. Another factor is clearly the strength of a possible Ti−E bond.

Other Possible Isomers. An isomer of the form H_2TiSiH_2, containing only terminal Ti−H and Si−H bonds, is calculated to have an energy which is 89.3 kJ mol^{-1} higher than that calculated for $HTi(\mu\text{-}H)_3Si$. In the case of H_2TiSnH_2, the energy difference amounts to 115.5 kJ mol^{-1} in favor of the isomer with three H bridges. The decreasing strength of the Ti−E bond down the group is probably responsible for the increasing energy of the H_2TiEH_2 isomer. The IR spectra recorded for the products of the reactions between Ti atoms and CH_4, SiH_4, or SnH_4 gave no evidence for the formation of these species.

Assignment of the Matrix Products. The combination of experimental and quantum-chemical results can now be used to identify and characterize most of the species formed in the course of our experiments.

$HTiCH_3$ (1). Photolysis is necessary to initiate a limited reaction between Ti and CH_4. The product yield is relatively small. Nevertheless, the appearance of a ν(Ti−H) band in the product spectrum indicates that some of the Ti atoms have indeed inserted into a C−H bond, leading in all probability to a species of the general formula $HTiCH_3$. The wavenumber argues for a Ti(II) species. The IR spectrum shows no absorption in the region between 1400 and 900 cm^{-1} that is characteristic of the $\nu(C-H_b)$ and $\nu(Ti-H_b)$ stretching modes of bridging H atoms (H_b). The obvious inference then is that product **1** contains only terminal H atoms. Our quantum-chemical calculations (see above) are in excellent agreement with these results. According to the calculations, $HTiCH_3$ features no bridging H atom. The calculations also agree that one vibrational mode carries most of the IR intensity. The wavenumber of this mode is calculated to be 1551.3 cm^{-1}, a value which compares well with the value of 1513.5 cm^{-1} that we observe. From a comparison with the measured IR spectrum, it is clear that $HTiCH_3$ is formed in its triplet electronic state in a spin-allowed reaction between Ti atoms and CH_4.

Ti·SiH_4 and Ti·SnH_4. The bands at 2164.3, 2160.4, 893.8, and 888.7 cm^{-1} in the experiments with SiH_4 and at 1881.8, 1876.7, 1870.7, 657.0, and 648.0 cm^{-1} in the experiments with SnH_4 can be assigned to a complex of the form Ti·EH_4. Unfortunately, it proved difficult to obtain information about the possible structures of such complexes Ti·SiH_4 and Ti·SnH_4 on the basis of quantum-chemical calculations. All attempts to model these species resulted in insertion of the Ti atom into one of the E−H bonds (E = Si, Sn). Thus, it appears that the barrier for insertion is very small. A detailed analysis of the energy hypersurface is difficult, because several electronic states have to be considered in these calculations. Possibly a tridentate complex is formed, such as that which is observed for the formally valence isoelectronic BH_4^- anion in the case of Ti(III) complexes.[2] The adoption of such a structure is also suggested by our proposed reaction pathway (see below).

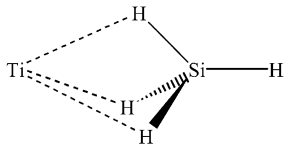

Possible structure of Ti·SiH_4

The wavenumbers observed for Ti·SiH_4 are close to those reported previously for Al·SiH_4.[19,20] In the case of Al·SiH_4, the binding energy of the complex was estimated to be not more than 10 kJ mol^{-1} on the basis of quantum-chemical calculations. The IR spectrum measured for Ti·SiH_4 thus indicates that this complex is also only weakly bound.

***cis*- and *trans*-$HTi(\mu\text{-}H)_2SiH$ (2aa and 2ab).** Our experiments clearly show that Ti atoms are much more reactive toward SiH_4 and SnH_4 than toward CH_4. Already, upon deposition, the IR spectra give evidence not only for the formation of the complex Ti·SiH_4 or Ti·SnH_4 but also for some degree of spontaneous insertion of the Ti atoms into the Si−H and Sn−H bonds, respectively.

On the basis of the IR spectra, both **2aa** and **2ab** are likely to have one terminal Ti−H bond and Ti−H−Si bridges. The spectra also indicate the presence of one terminal Si−H bond. The obvious inference is that **2aa** and **2ab** are *cis*- and *trans*-$HTi(\mu\text{-}H)_2SiH$.

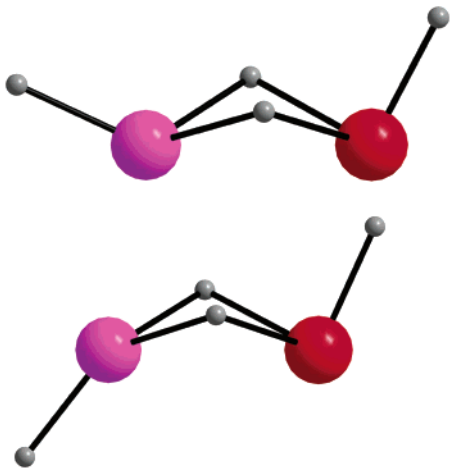

Table 6. Comparison between Observed and Calculated Wavenumbers (in cm^{-1}, with Intensities (in km mol^{-1}) Given in Parentheses) for HTi(μ-H)$_2$SiH and DTi(μ-D)$_2$SiD (2aa (Cis) and 2ab (Trans))]

HTi(μ-H)$_2$SiH (cis)		DTi(μ-D)$_2$SiD (cis)		approx descripn of molecular motion
obsd	calcd	obsd	calcd	
2055.0/2047.4	2075.6 (149)	1480.5	1499.2 (78)	ν(Si−H$_t$)
	1575.2 (90)		1132.8 (46)	ν_s(Si−H$_b$)
1541.5	1564.2 (206)	1125.6	1127.5 (106)	ν_{as}(Si−H$_b$)
1507.2	1522.3 (424)	1085.6	1091.3 (227)	ν(Ti−H$_t$)
1144.5	1171.2 (197)	829.3	839.8 (97)	ν_s(Ti−H$_b$)
	1105.2 (1)		787.2 (0.2)	ν_{as}(Ti−H$_b$)
854.0	814.2 (31)	634.7	593.1 (14)	δ(H$_t$−Si−H$_b$)
	608.3 (0.01)		445.2 (0.2)	
	512.1 (10)		401.0 (9)	
	317.3 (20)		290.6 (12)	ν(Si−Ti)
	196.1 (277)		142.7 (146)	
	155.0 (137)		113.0 (72)	torsion
HTi(μ-H)$_2$SiH (trans)		DTi(μ-D)$_2$SiD (trans)		approx descripn of molecular motion
obsd	calcd	obsd	calcd	
2042.5/2040.5	2121.7 (105)	1495.5/1490.8	1533.4 (56)	ν(Si−H$_t$)
	1641.0 (68)		1179.8 (37)	ν_s(Si−H$_b$)
	1628.4 (159)		1173.3 (82)	ν_{as}(Si−H$_b$)
1514.1	1530.8 (404)	1090.5	1096.9 (215)	ν(Ti−H$_t$)
1120.7	1045.7 (204)		753.6 (95)	ν_s(Ti−H$_b$)
	986.3 (2)		702.8 (1)	ν_{as}(Ti−H$_b$)
937.8/934.2	849.7 (58)		614.8 (29)	δ(H$_t$−Si−H$_b$)
	564.9 (3)		415.8 (2)	
	430.5 (6)		375.9 (19)	
	336.8 (30)		276.1 (11)	ν(Si−Ti)
	191.7 (240)		140.7 (125)	
	160.4 (130)		115.2 (67)	torsion

Table 6 compares the experimentally observed wavenumbers with those forecast by our DFT calculations. The mode which can roughly be described as ν(Si−H$_t$) is calculated to occur at 2075.6 cm^{-1} in the case of *cis*-HTi(μ-H)$_2$SiH and at 2121.7 cm^{-1} in the case of the trans isomer. These values compare well with the experimentally obtained values of ca. 2052 and ca. 2042 cm^{-1}, respectively. The ν(H):ν(D) ratios are also in agreement with this assignment (calculated 1.3845:1 and observed 1.3855:1 for the cis form and calculated 1.3837:1 and observed 1.3672:1 for the trans form). The next two modes calculated at 1575.2 and 1564.2 cm^{-1} for the cis form and at 1641.0 and 1628.4 cm^{-1} for the trans form are strongly associated with the symmetric and antisymmetric Si−H$_b$ stretching modes, ν_s(Si−H$_b$) and ν_{as}(Si−H$_b$). Unfortunately, our experiments found only one of these modes, ν_{as}(Si−H$_b$), of the cis form. This mode should have the highest intensity of the three ν(Si−H) modes, according to the calculations. Moving to lower wavenumber, the next vibrational mode has a high contribution from ν(Ti−H$_t$). This mode is calculated to have a wavenumber of 1522.3 cm^{-1} for the cis form and 1530.8 cm^{-1} for the trans form. The experimental values of 1507.2 and 1514.1 cm^{-1} are in excellent agreement with the calculated values. As expected, the ν(H)/ν(D) ratios are close to 1.4:1 for this mode (cis, calculated 1.3949:1, experimental 1.3884; trans, calculated 1.3956, experimental 1.3884). The symmetric and antisymmetric ν(Ti−H$_b$) modes contribute to the next two modes, which are predicted to appear at 1171.2 and 1105.2 cm^{-1} for *cis*-HTi(μ-H)$_2$SiH and at 1045.7 and 986.3 cm^{-1} for the trans form. One of these modes is calculated to have a very low intensity, and therefore, it is not surprising that the experiments gave evidence for only one of the two transitions. This was located at 1144.5 and 1120.7 cm^{-1} for the cis and trans forms, respectively.

We strictly cannot rule out the possibility that the presence of the bands assigned to **2aa** and **2ab** results from a matrix splitting. This would imply that only one of the two isomers (*cis*- or *trans*-HTi(μ-H)$_2$SiH) is formed. However, because of the similar energies, we believe that it is more likely that **2aa** and **2ab** are the cis and trans isomers.

In the case of the Sn homologues, the experiments failed to find any evidence for a ν(Sn−H) stretching fundamental, which is calculated to occur at 1667.3 and 1661.1 cm^{-1} for *cis*- and *trans*-HTi(μ-H)$_2$SnH, respectively, and should carry sufficient intensity. Thus, we conclude that HTi(μ-H)$_2$SnH is not formed. According to the calculations, the energy difference between the global energy minimum form of TiSnH$_4$, HTi(μ-H)$_3$Sn (see below), and *cis*- and *trans*-HTi(μ-H)$_2$SnH amounts to more than 50 kJ mol^{-1}. In the case of the Si homologue, the difference was less than half this value (24−25 kJ mol^{-1}). The relative destabilization of HTi(μ-H)$_2$SnH might explain the fact that HTi(μ-H)$_2$SiH but not HTi(μ-H)$_2$SnH can be found in our experiments.

HTi(μ-H)$_3$Si and HTi(μ-H)$_3$Sn (3a and 3b). According to our calculations, these species define the global energy minima for molecules with the overall formula TiSiH$_4$ and TiSnH$_4$. The measured IR spectra leave no doubt that both are formed in our experiments. They are already present upon deposition but can be formed in higher concentrations following appropriate photolysis. While HTi(μ-H)$_3$Si can be decomposed upon photolysis with broad-band visible light (a possible decomposition product being TiSiH$_2$), HTi(μ-H)$_3$Sn is photostable. As already mentioned, both species exhibit a triplet ground electronic state.

Table 7. Comparison between Observed and Calculated Wavenumbers (in cm^{-1}, with Intensity (in km mol^{-1}) Given in Parentheses) for HTi(μ-H)$_3$Si and DTi(μ-D)$_3$Si (3a)

HTi(μ-H)$_3$Si		DTi(μ-D)$_3$Si		approx descripn of molecular motion
obsd	calcd	obsd	calcd	
	1698.2 (79)		1222.0 (44)	ν_s(Si−H$_b$)
1524.8	1557.3 (222)	1098.3	1120.0 (86)	ν(Ti−H$_t$) (+ν_s(Si−H$_b$))
1509.2	1546.5 (158)	1087.2	1110.1 (88)	ν_{as}(Si−H$_b$)
1498.1	1542.3 (148)	1079.7	1108.4 (106)	ν_s(Si−H$_b$) (+ν(Ti−H$_t$))
1129.7	1129.8 (398)	831.3	818.2 (211)	ν(Ti−H$_b$)
	1083.8 (54)		775.3 (19)	ν(Ti−H$_b$)
	1045.0 (19)		747.6 (8)	ν(Ti−H$_b$)
	743.0 (31)		535.6 (17)	Ti(μ-H)$_3$Si def
	721.0 (13)		518.2 (6)	Ti(μ-H)$_3$Si def
	361.8 (51)		345.6 (16)	ν(Ti−Si)
	256.4 (136)		192.1 (83)	δ(Si−Ti−H$_t$)
	232.2 (87)		167.2 (47)	torsion

Table 8. Comparison between Observed and Calculated Wavenumbers (in cm^{-1}, with Intensity (in km mol^{-1}) Given in Parentheses) for HTi(μ-H)$_3$Sn and DTi(μ-D)$_3$Sn (3b)

HTi(μ-H)$_3$Sn		DTi(μ-D)$_3$Sn		approx descripn of molecular motion
obsd	calcd	obsd	calcd	
1478.4	1520.0 (484)	1065.0	1089.9 (256)	ν(Ti−H$_t$)
	1302.6 (97)	939.9	928.0 (50)	ν_s(Sn−H$_b$)
	1207.2 (104)	905.5	860.2 (50)	ν_{as}(Sn−H$_b$)
1021.2	1166.0 (168)		831.2 (87)	ν_s(Sn−H$_b$)
1016.5	1063.3 (457)	741.3	759.7 (239)	ν(Ti−H$_b$)
	940.5 (154)		672.2 (73)	ν(Ti−H$_b$)
	917.5 (47)		656.4 (22)	ν(Ti−H$_b$)
624.8	656.1 (41)	452.0	468.9 (21)	Ti(μ-H)$_3$Sn def
	559.4 (89)		402.2 (48)	Ti(μ-H)$_3$Sn def
255.8	254.7 (87)		238.4 (11)	ν(Ti−Sn)
	195.5 (94)	183.2	148.3 (109)	δ(Sn−Ti−H$_t$)
	192.0 (141)		139.7 (46)	torsion

In Tables 7 and 8, the calculated IR properties are compared with the observed ones for HTi(μ-H)$_3$E and DTi(μ-D)$_3$E. The tables also contain attempts to describe the modes responsible for the absorptions. Obviously, in the absence of symmetry higher than C_s, there is a high degree of coupling. The mode coupling is especially strong between ν(Ti−H$_t$) and some of the ν(Si−H$_b$) vibrations. The mode with the highest contribution from Ti−H$_t$ stretching is located at 1557.3 and 1520.0 cm^{-1} for HTi(μ-H)$_3$Si and HTi(μ-H)$_3$Sn, respectively. The observed wavenumbers of 1524.8 and 1478.4 cm^{-1}, respectively, are in pleasing agreement with the calculated values. The ν(H):ν(D) ratios amount to 1.3904:1 and 1.3946:1 for the calculated wavenumbers and 1.3883:1 and 1.3882:1 for the observed values.

The wavenumbers of the three fundamentals with high Si−H$_b$ stretching character are located at 1698.2, 1546.5, and 1542.3 cm^{-1}. The band at 1698.2 cm^{-1} is calculated to be much weaker than the other two, and unfortunately, our experiments have failed to detect it. However, the other two modes appear clearly in the experimental IR spectra at 1509.2 and 1498.1 cm^{-1}. The strong, sharp band at 1498.1 cm^{-1} in the observed spectrum and 1542.3 cm^{-1} in the calculated spectrum belongs to a mode which also includes a very high contribution from Ti−H$_b$ stretching (almost as high as in the mode calculated to occur at 1557.3 cm^{-1}). In the case of the Sn homologue, the modes with high ν(Sn−H$_b$) stretching character occur at significantly lower wavenumbers and, consequently, the coupling with ν(Ti−H$_t$) is reduced. These modes are, however, in close proximity to fundamentals with a high contribution from the three ν(Ti−H$_b$) stretching fundamentals, which results in extensive and complicated mode coupling.

Next in order of decreasing wavenumber follow the three vibrations with high ν(Ti−H$_b$) character. For both the Si- and Sn-containing compounds, one of these three modes dominates in intensity. This mode is calculated to occur at 1129.8 and 1063.3 cm^{-1}, respectively. The experiments give evidence for intense absorptions at 1129.7 and 1016.5 cm^{-1}. The ν(H):ν(D) ratios of 1.3808:1 and 1.3996:1 derived from the quantum-chemical calculations compare well with the values of 1.3590:1 and 1.3712:1 afforded by experiment.

The modes that can be described as ν(Ti···Si) and ν(Ti···Sn) vibrations are calculated to give rise to relatively weak features at 361.8 and 254.7 cm^{-1}. Unfortunately, our experiments fail to detect these bands.

HTi(μ-H)$_2$(H)Sn (4ba and 4bb). These species are clearly precursors to HTi(μ-H)$_3$Sn. Their absorptions lie close to those of HTi(μ-H)$_3$Sn and, hence, indicate that **4ba** and **4bb** feature a terminal Ti−H bond and one or more bridging H atoms. From the absence of an absorption with a high degree of Sn−H$_t$ stretching, we can conclude that **4ba** and **4bb** probably do not contain any terminal Sn−H bonds. The best explanation in our view is that **4ba** and **4bb** are species with a structure that lies between those of *cis*- or *trans*-HTi(μ-H)$_3$SnH and HTi(μ-H)$_3$Sn, in which the three H atoms are already in more or less bridging positions, but the terminal Ti−H bond has not relaxed to its optimal position. It is certainly not easy to calculate the detailed structure of such a species, and more sophisticated methods are definitely required for any future attempt.

Reaction Pathways. The experiments clearly show that the reactions between Ti atoms and SiH$_4$ or SnH$_4$ proceed spontaneously, while the reaction between Ti and CH$_4$ requires the action of photolysis and even then proceeds inefficiently. Thus, SiH$_4$ and SnH$_4$ appear much more reactive toward Ti atoms than does CH$_4$.

The reaction with SiH$_4$ proceeds first to the weakly bound complex Ti·SiH$_4$, in which the SiH$_4$ is possibly η^3 coordinated (see eq 1). This complex can be converted with almost no activation energy into *cis*- and *trans*-HTi(μ-H)$_2$SiH and subsequently to HTi(μ-H)$_3$Si, all of which are observed in the infrared spectrum of the matrix following deposition. *cis*- and *trans*-HTi(μ-H)$_2$SiH may also be converted to HTi(μ-H)$_3$Si by the action of

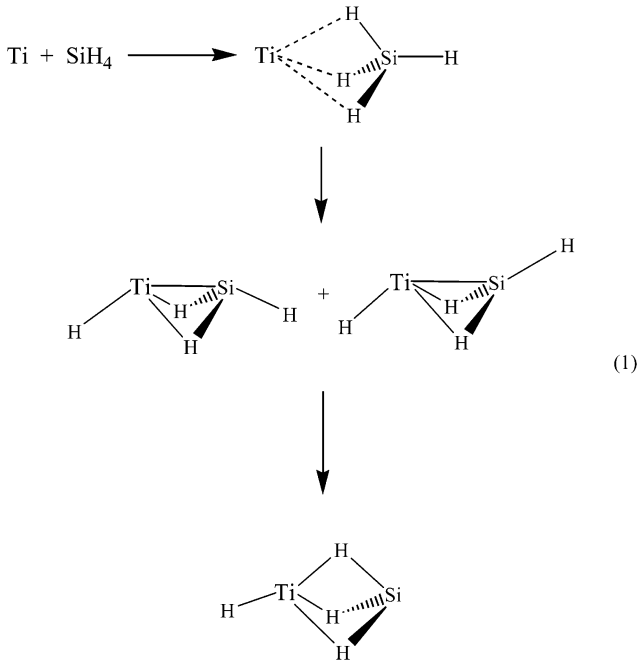

photolysis at $\lambda_{max} = 410$ nm. Such a reaction is calculated to be exothermic by 24.3 kJ mol^{-1} (cis) and 24.7 kJ mol^{-1} (trans).

According to our calculations, the overall reaction between Ti and SiH_4 to give $HTi(\mu\text{-}H)_3Si$ is exothermic by −154.6 kJ mol^{-1}, while the reaction between Ti atoms and SnH_4 proceeds with a reaction energy of −266.0 kJ mol^{-1}. In contrast, the reaction between Ti atoms and CH_4 to give $HTiCH_3$ (eq 2) is exothermic by

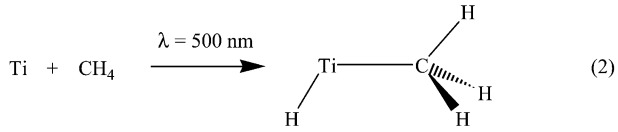

only −92.3 kJ mol^{-1}. All these values have to be treated with caution, however, since they clearly depend on the method and basis set used in the calculations. All the reactions are spin allowed.

The reaction of Ti with SnH_4 leads to an end product analogous to that delivered by the reaction with SiH_4. However, *cis*- and *trans*-$HTi(\mu\text{-}H)_2SnH$ appear not to be formed. Instead, the IR spectra point to intermediates which should have structures featuring both fully established Ti−H−Sn bridges and Ti···H−Sn interactions.

The experiments show that visible light leads to the slow decomposition of $HTi(\mu\text{-}H)_3Si$. Unfortunately, it was not possible to identify the decomposition products. One possible product is $TiSiH_2$. We also cannot rule out the possibility of decomposition back to Ti atoms and SiH_4. Finally, hydrides such as TiH_2 and SiH_2 might be possible decomposition products. However, no absorptions which had previously been assigned to these two species[31,32] were detected in the experiments.

Conclusions

This account describes studies of the spontaneous and photolytically activated reactions of Ti atoms with CH_4, SiH_4, and SnH_4 in Ar matrixes at 12 K. The results show that the reactivities of Ti atoms toward the three reactants are very different. In the case of CH_4, the reaction requires photolytic activation of the Ti atoms and then proceeds to give $HTiCH_3$, a species featuring only terminal Ti−H and C−H bonds. With SiH_4 and SnH_4, spontaneous reactions were observed. For SiH_4, the products of these reactions are the weakly bound complex Ti·SiH_4, the species *cis*- and *trans*-$HTi(\mu\text{-}H)_2SiH$ with two bridging H atoms, and $HTi(\mu\text{-}H)_3Si$ with three bridging H atoms. $TiSiH_4$ can be converted into *cis*- and *trans*-$HTi(\mu\text{-}H)_2SiH$ by the action of photolysis at $\lambda_{max} = 500$ nm. On photolysis at $\lambda_{max} = 410$ nm, *cis*- and *trans*-$HTi(\mu\text{-}H)_2SiH$ are themselves photolabile and undergo conversion into $HTi(\mu\text{-}H)_3Si$. According to quantum-chemical calculations, $HTi(\mu\text{-}H)_3Si$ defines the global energy minimum for all molecules of the general formula $TiSiH_4$. The reaction of Ti atoms with SnH_4 leads spontaneously to the complex Ti·SnH_4 and $HTi(\mu\text{-}H)_3Sn$ with three H bridges. Again, photolysis at $\lambda_{max} = 500$ and 410 nm can be used to increase the yield of $HTi(\mu\text{-}H)_3Sn$ at the expense of Ti·SnH_4. The mechanisms of the reactions and the structures of the products identified and characterized in this work may have wider significance in improving the understanding of oxidative-addition processes in catalytic cycles.

Acknowledgment. We thank (i) the *Deutsche Forschungsgemeinschaft* and the *Fonds der Chemischen Industrie* for financial support and (ii) Dr. Ingo Krossing for fruitful discussions.

OM040016O

(31) Chertihin, G. V.; Andrews, L. *J. Am. Chem. Soc.* **1994**, *116*, 8322.
(32) Andrews, L.; Wang, X. *J. Phys. Chem. A* **2002**, *106*, 7696.